

RPA1A-LP: TCGTTTCCTCATTTCAGATGG RPA1A-RP: TCGACCTTGGTATGGATTGAG	RPA2B-LP: ATGTGGTCAGCGAATCATTTTC RPA2B-RP: CGTTAGCAGTCGATTTGAAGC
RPA1B-LP: CTTCCAACCCAAGAAGAACTG RPA1B-RP: TCACAGGCCCTGTTACAATTC	ATR-LP: GCAGCAAAAATTTCTTGTTG ATR-RP: ACTTCAAGGGTCCGATGTTC
RPA1C-LP: CTTGTGGCTCACTCATAAGGG RPA1C-RP: ATATGTCAGGCCGAAGTGTTG	STN1-LP: GTGCCAGATTCATTGGAAAAC STN1-RP: AAAGCAAAAGGGAAAGGTGAG
RPA1D-LP: TCTCCGCTCTTACTGTCCAAG RPA1D-RP: ATCAAACAAAACAAAATGCGC	CTC1-LP: TATACCCCGTTCCAAGAATCC CTC1-RP: CTTTAGTCCTCCGTGGGATC
RPA1E-LP: TAAGAGCCACCCATGTACTGC RPA1E-RP: ATATGTCAGGCCGAAGTGTTG	RTEL1-LP: CCTTTTTGTGCTATGTCCAGC RTEL1-RP: CAAGAGAGCTTCACAAGGACG
RPA2A-LP: CTACGAATCCTCCTCCTCCAC RPA2A-RP: GATCCACCTTGAAATGTGGTG	LBb1.3: ATTTTGCCGATTTCGGAAC LBa1: TGGTTCACGTAGTGGGCCATCG

Supplementary Table S1. List of PCR genotyping primers used to isolate homozygous T-DNA insertion lines. Signal Salk (<http://signal.salk.edu/tdnaprimers.2.html>) generated gene-specific primers and a T-DNA left border primer, LBb1.3 (for all SALK lines except *atr*) or LBa1 (for *atr*), were used for PCR based genotyping.

A

	Mean telomere length (Kb)					
Generation (G)	WT	<i>rpa1a</i>	<i>rpa1b</i>	<i>rpa1c</i>	<i>rpa1d</i>	<i>rpa1e</i>
G1	3.05	3.04	3.00	3.10	2.98	3.08
G2	3.21	3.16	3.10	3.20	3.16	3.15
G3	3.16	3.30	2.91	2.98	3.34	3.20
Grand mean (G1 - G3)	3.14	3.17	3.00	3.09	3.16	3.15

B

	Mean telomere length (Kb)
Generation (G)	<i>rpa1b rpa1d</i>
G1	1.53
G2	1.48
G3	1.50
G4	1.47
G5	1.49
G6	1.48
G7	1.49
Grand Mean TRF (G1 – G7)	1.49

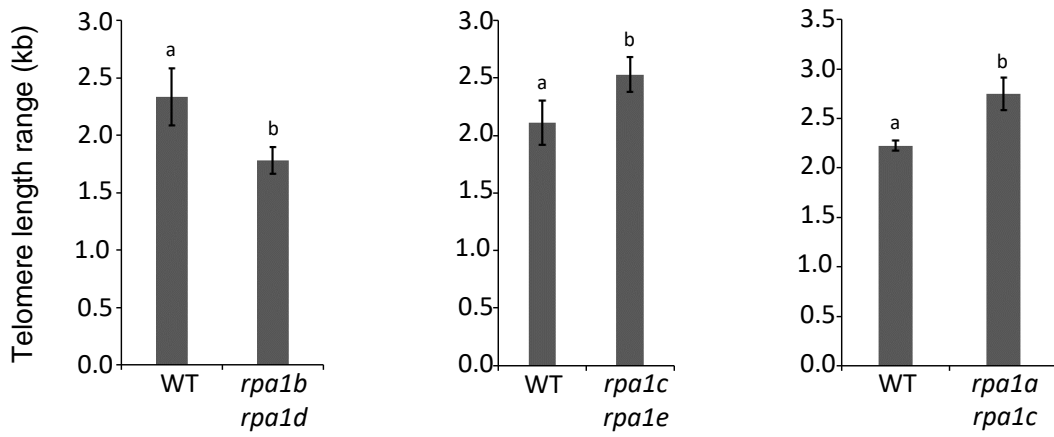
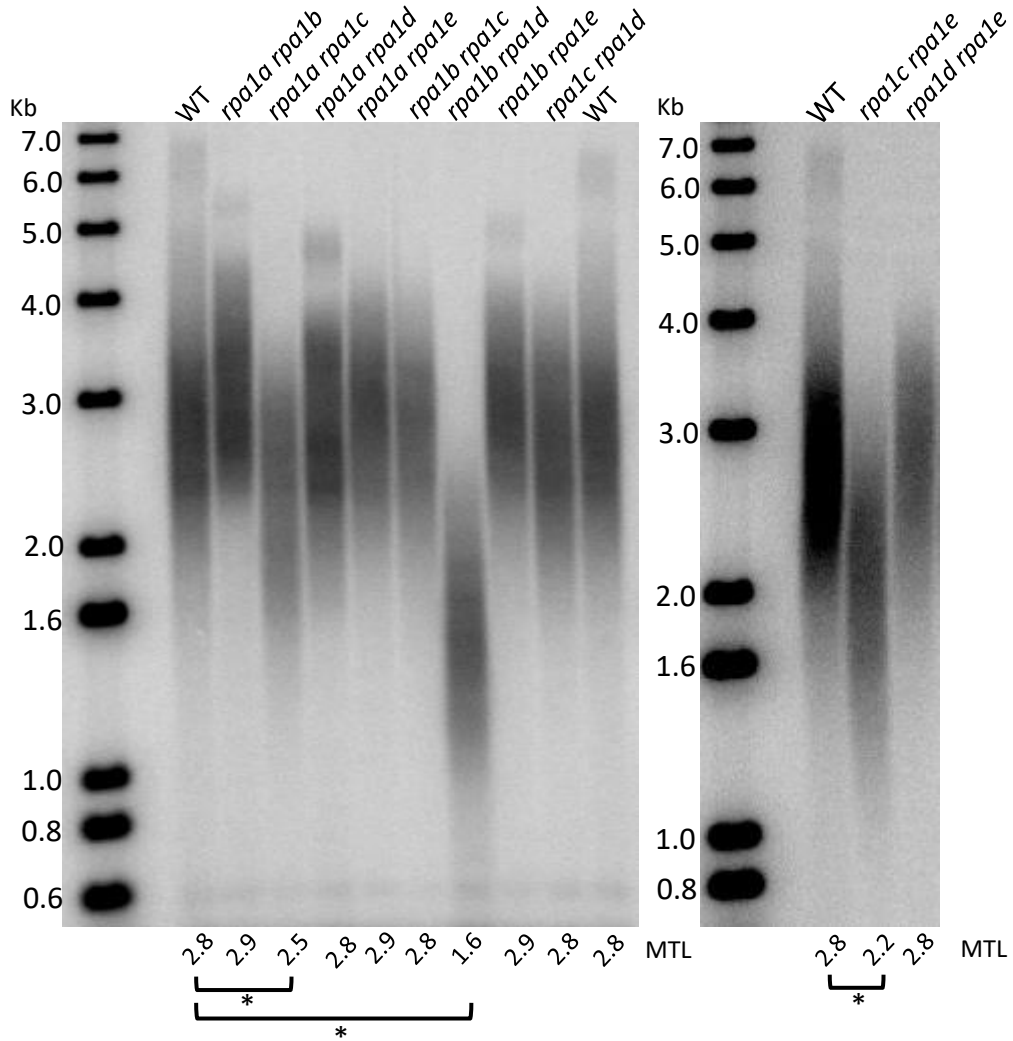
C

	Mean telomere length (Kb)
Generation (G)	<i>rpa1c rpa1e</i>
G1	2.23
G2	2.20
G3	2.20
G4	2.19
G5	2.16
G6	2.16
G7	2.21
Grand Mean TRF (G1 – G7)	2.19

D

Generation (G)	Mean telomere length (Kb)	
	<i>rpa2a</i>	<i>rpa2b</i>
G1	1.76	3.00
G2	1.53	2.99
G3	1.59	3.04
Grand mean (G1 - G3)	1.63	3.01

Supplementary Table S2. RPA mutant telomere length data. Mean telomere length measurements obtained from TRF analysis for *rpa1* single mutants (A), *rpa1b rpa1d* (B), *rpa1c rpa1e* (C), and *rpa2a* and *rpa2b* single mutants (D). Mean telomere length data of individual generation (G) is calculated from results of three biological replicates.

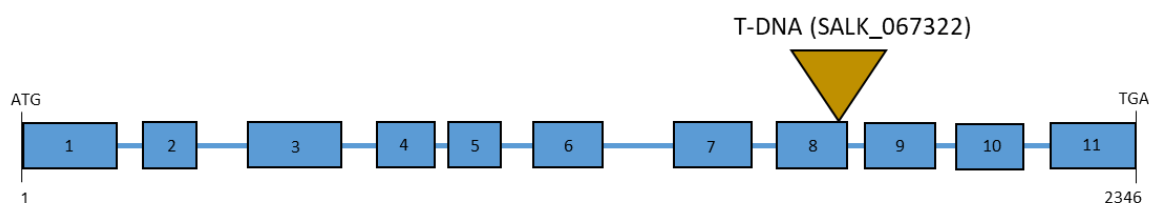
A**B**

Supplementary Figure S1. Telomere length analysis of RPA1 mutant combinations. (A) Telomere length range varies among the different RPA1 double mutant (*rpa1b rpa1d* [replication]; *rpa1c rpa1e* [repair], and *rpa1a rpa1c* [meiosis]) groups. Range analysis was based on TRF data that was used to generate figure 1. Figures show mean telomere length range and standard deviation. Different Letters above bars denote statistically significant difference at $P \leq 0.05$ (unpaired T-test). (B) Double mutants of *rpa1* (a-e), other than the replication (*rpa1b rpa1d*), repair (*rpa1c rpa1e*), and meiotic recombination (*rpa1a rpa1e*) do not show telomere length change. Each lane represents telomeres extracted from ten, 20-day-old plants. Numbers below TRF images represent mean telomere lengths (MTL) in kb from two biological replicates. Raw data are shown only for one of these replicates. All of the plants in the figure represent G2 generation except for *rpa1a rpa1c*, which are G1 as the double mutant is completely sterile (Aklilu *et al.* 2014). For analysis of statistical MTL difference, we did pairwise comparisons of each mutant against WT using unpaired T-test. Asterisk show a statistically significant difference at $P \leq 0.05$.

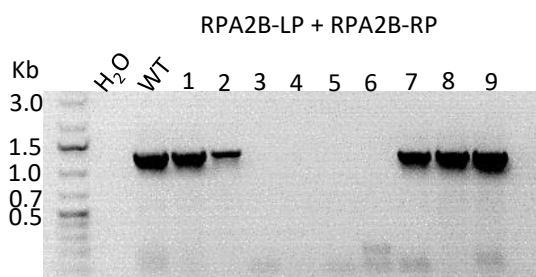
A

Score	Expect	Method	Identities	Positives	Gaps
160 bits(405)	3e-53	Compositional matrix adjust.	91/227(40%)	137/227(60%)	13/227(5%)
RPA2A 7	FEPNSGFSGGFMSSQPS-QAYESSSSSTAKNRDFQGLVPVTVKQITECFQSSGGEKSGGLVI	65	F+ N+ F+GGGFM SQ + QA+ESSSS KNRD + L+P+T+KQ++ ++GE S I		
RPA2B 6	FDGNAAFAGGGFMPSQATTQAHESSSS-LKNRDVRTLLPLTLKQLSSA-STTGE-SNFSI	62			
RPA2A 66	NGISLTNVSLVGLVCDKDESKVTEVRFLLDDGTGRIDCKRWVSETFDAREMESVRDGTIV	125	+G+ + V +VG + + E+++T+V F +DDGTG +DC RW + EME+V+ G YV		
RPA2B 63	DGVDIKTVIVGRI-SRMENRITQVDFVDDGTGWVDCVRWCHARQETEEMEAVKLGMYV	121			
RPA2A 126	RLSGHLKTFQGKTQLLVFSVRPIMDFNEVTFHYIECIHFYSONSESQRQQVGDVTQSVNT	185	RL GHLK FQ GK + VFSVRP+ DFNE+ H+ EC++ + N+ + + G +TQ T		
RPA2B 122	RLHGHLLKIFQGKRSVNVFSVRPVTDFNEIVHHFTECMYVHMYNT---KLRGGSITQDTAT	178			
RPA2A 186	TFQGSNTNQATLLNPVSSQNNDGNGRKN-----LDDMILDYLKQP	227	+ T P + +N + N + +L+YL QP		
RPA2B 179	PRPQMPYSTMPPTPAKPYQTGPSNQFPNQFNDSMHGVKQTVLNYLNQP	225			

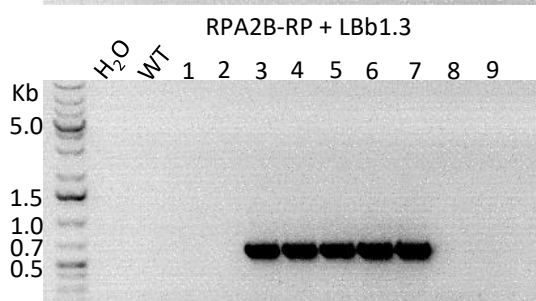
B



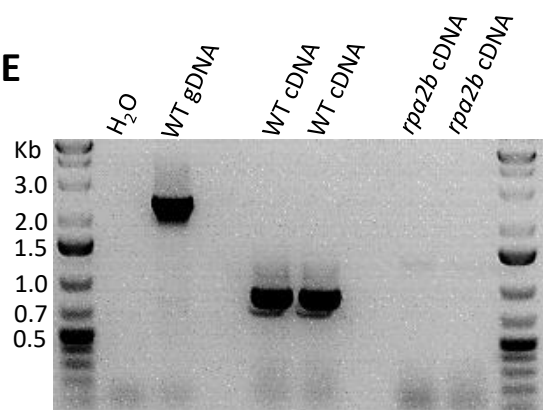
C



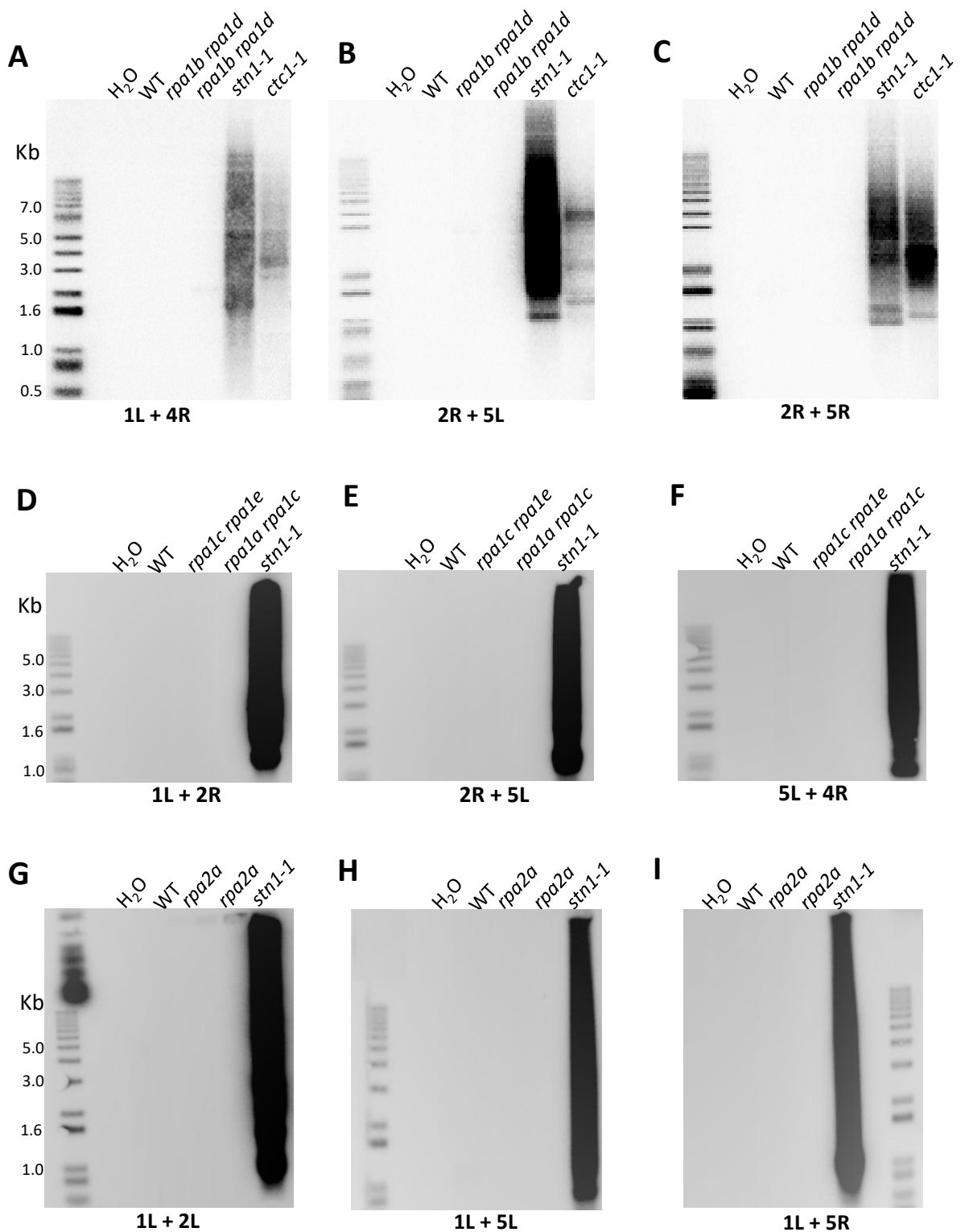
D



E

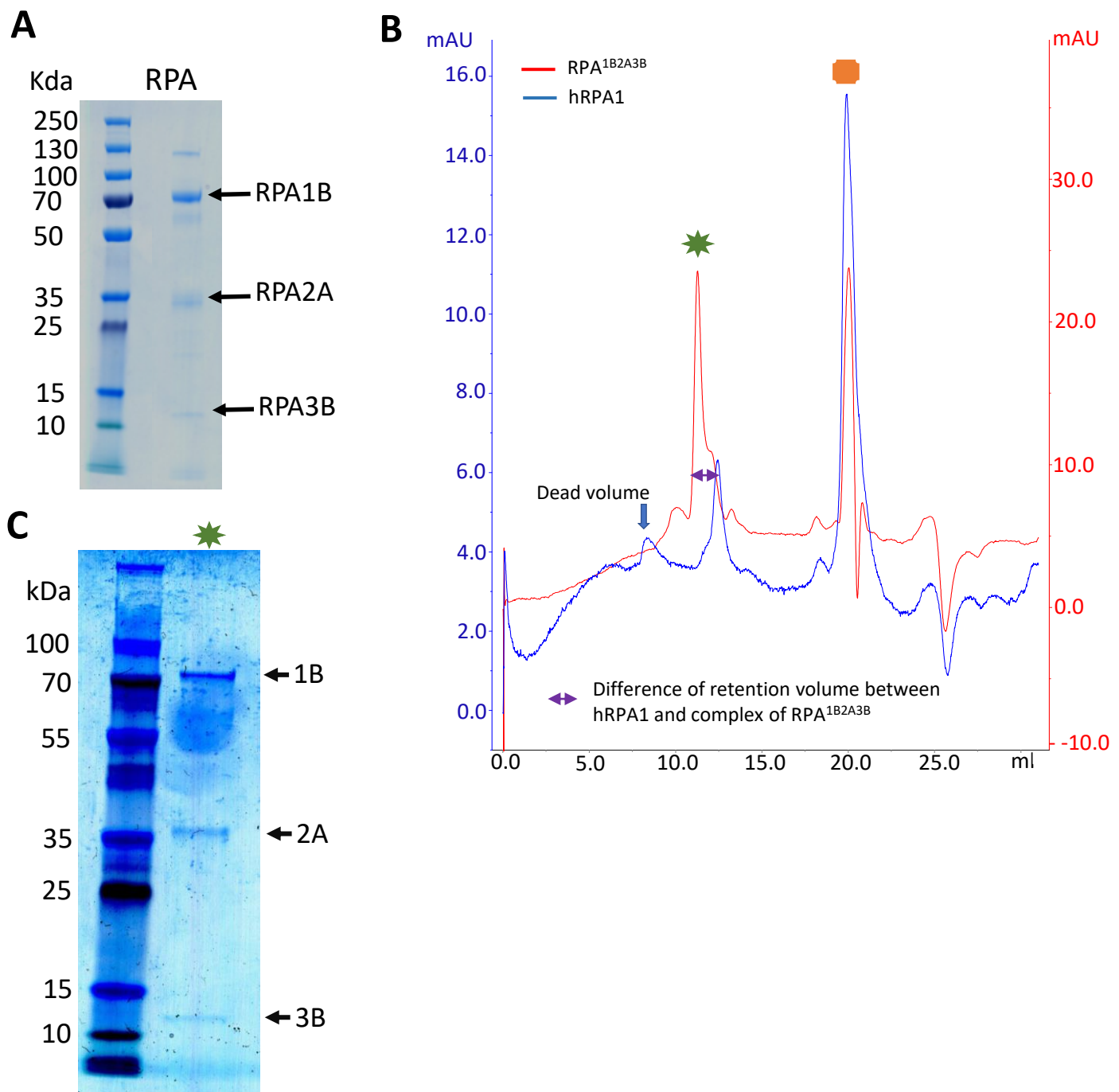


Supplementary Figure S2. *rpa2b-1* (SALK_067322) is a null mutant. (A) RPA2A and RPA2B amino acid alignment conducted using NCBI BLASTp. The two proteins show 40% and 60 % amino acid sequence identity and similarity, respectively. (B) T-DNA insertion site for *rpa2b-1*. Boxes and lines represent exons and introns, respectively. (C and D) PCR genotyping result for the *rpa2b-1* T-DNA insertion mutant line. Lanes: H2O and WT: water and wild type control, respectively; (1,2,8,9), WT plants; (3,4, 5,6), *rpa2b-1* homozygous mutant plants; (7), *rpa2b-1* heterozygous plant. RPA2B-LP: gene specific (RPA2B) left primer; RPA2B-RP: gene specific (RPA2B) right primer; LBb1.3: T-DNA specific left border primer. Expected PCR product length for RPA2B-LP + RPA2B-RP and RPA2B-RP + LBb1.3 primer combinations are 1217 bp and 545-845 bp, respectively. (E) RT-PCR analysis in *rpa2b-1* mutants. Total RNA was extracted from 7-day-old seedlings and used for cDNA synthesis followed by PCR amplification (40 cycles) using RPA2B primers. gDNA = genomic DNA. A 1 kb plus DNA ladder is used as a size marker.



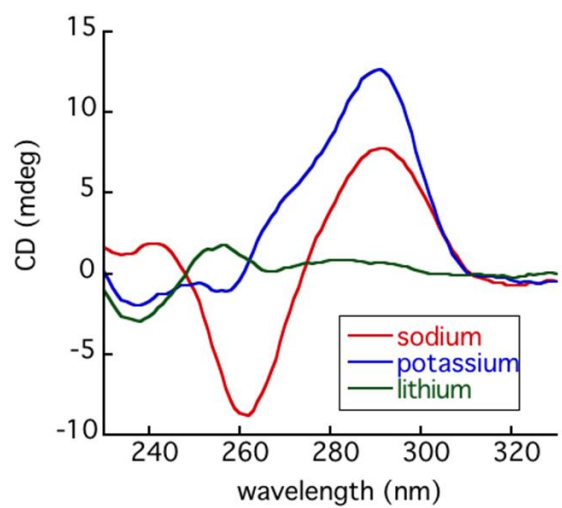
Supplementary Figure S3. Telomeres are not prone to end-to-end fusion in *rpa* mutants. (A-I)

Telomere fusion PCR reactions with DNA from *rpa1b rpa1d* (A-C), *rpa1c rpa1e* and *rpa1a rpa1c* (D-E), and *rpa2a* (G-I) mutants. DNA from *stn1-1* and *ctc1-1* was used as positive controls (Song *et al.* 2008; Surovtseva *et al.* 2009). Numbers and letters below each figure indicate PCR primers used for specific chromosome number and Left (L) or right (R) chromosome arm.

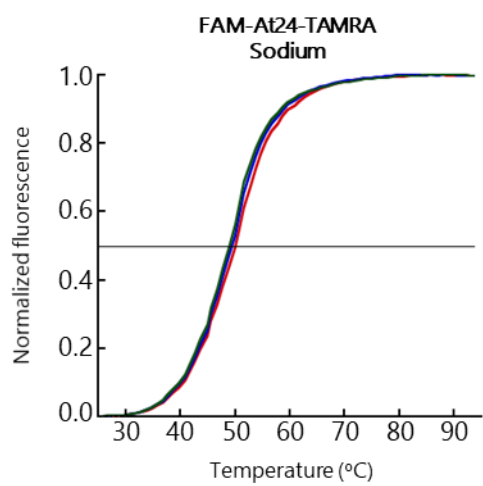


Supplementary Figure S4. Recombinant RPA^{1B2A3B} forms a heterotrimeric protein complex. (A) Coomassie-blue stained SDS-PAGE of recombinant RPA^{1B2A3B}. The protein is estimated to be 80–90% pure. While other unknown proteins co-purify with the potential to bind and unfold G4 DNA, the major protein that binds ssDNA in *E. coli* is the single-stranded binding (SSB) protein, a tetramer of 4*18.8 (Meyer and Laine 1990). There is no band corresponding to the 18.8 kDa monomer. (B) Size-exclusion chromatography to check for formation of a heterotrimeric RPA^{1B2A3B} complex (—). The human RPA subunit 1 (hRPA1) (—) retention volume on this column was used as a weight marker to compare with RPA^{1B2A3B}. Chromatography of RPA^{1B2A3B} showed an absorption peak of 11 mL retention volume while hRPA1 showed a peak of 13 mL retention volume. The result indicates that a complex of Arabidopsis RPA^{1B2A3B} proteins formed as its weight is bigger than hRPA1. Fractions containing this complex (★) were concentrated and analyzed on SDS-PAGE stained with Coomassie-blue (C). This revealed three bands corresponding to RPA1B, RPA2A and RPA3B, indicating that the heterotrimeric complex is formed. We noticed an absorption peak at the end of both chromatography of 20 mL retention volume (■), but analysis of this fraction on SDS-PAGE showed no bands (data not shown), suggesting that it does not correspond to a protein sample.

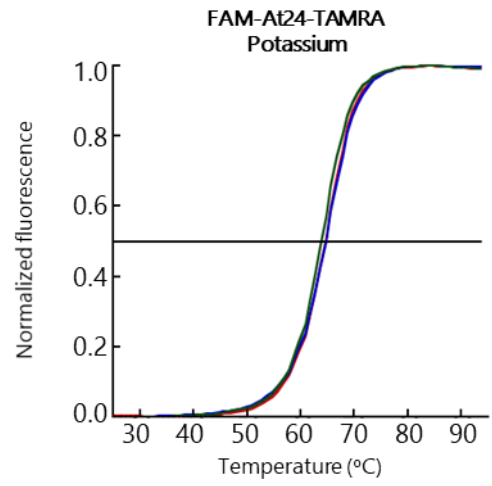
A



B

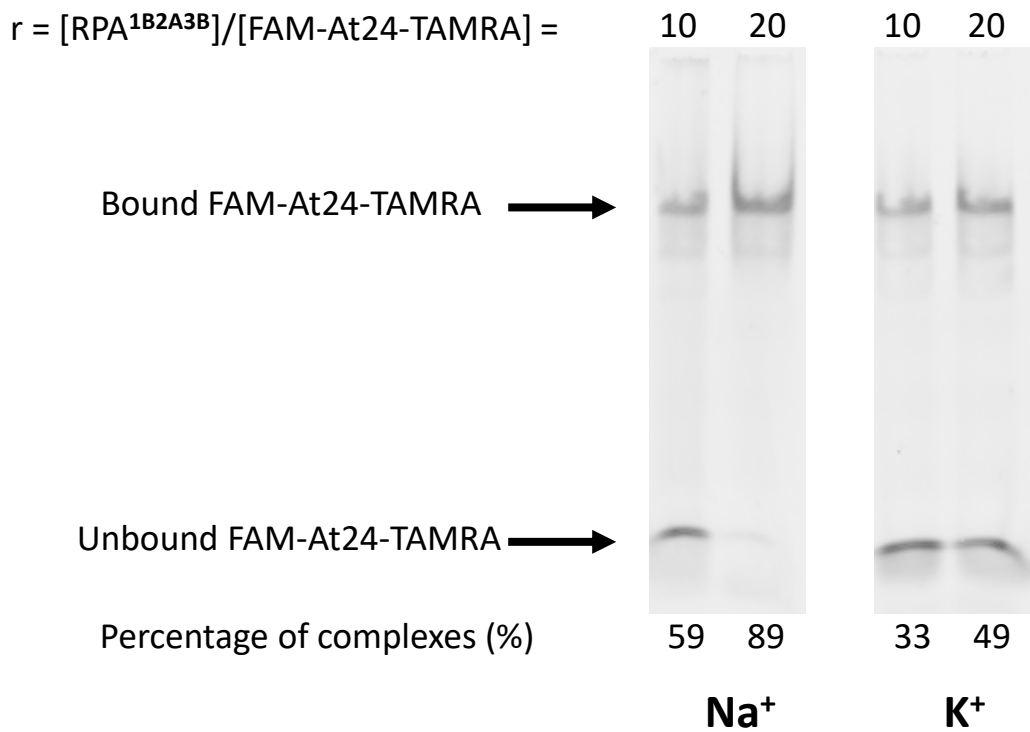


C

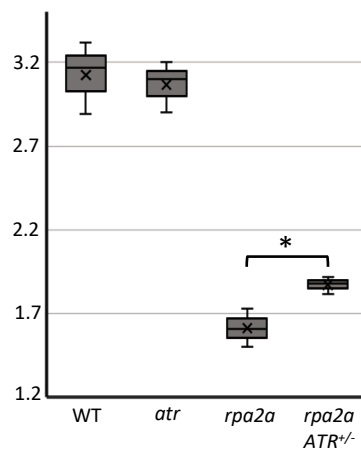


	FAM-At24-TAMARA	
	Sodium	Potassium
T _{1/2} (°C)	50	65

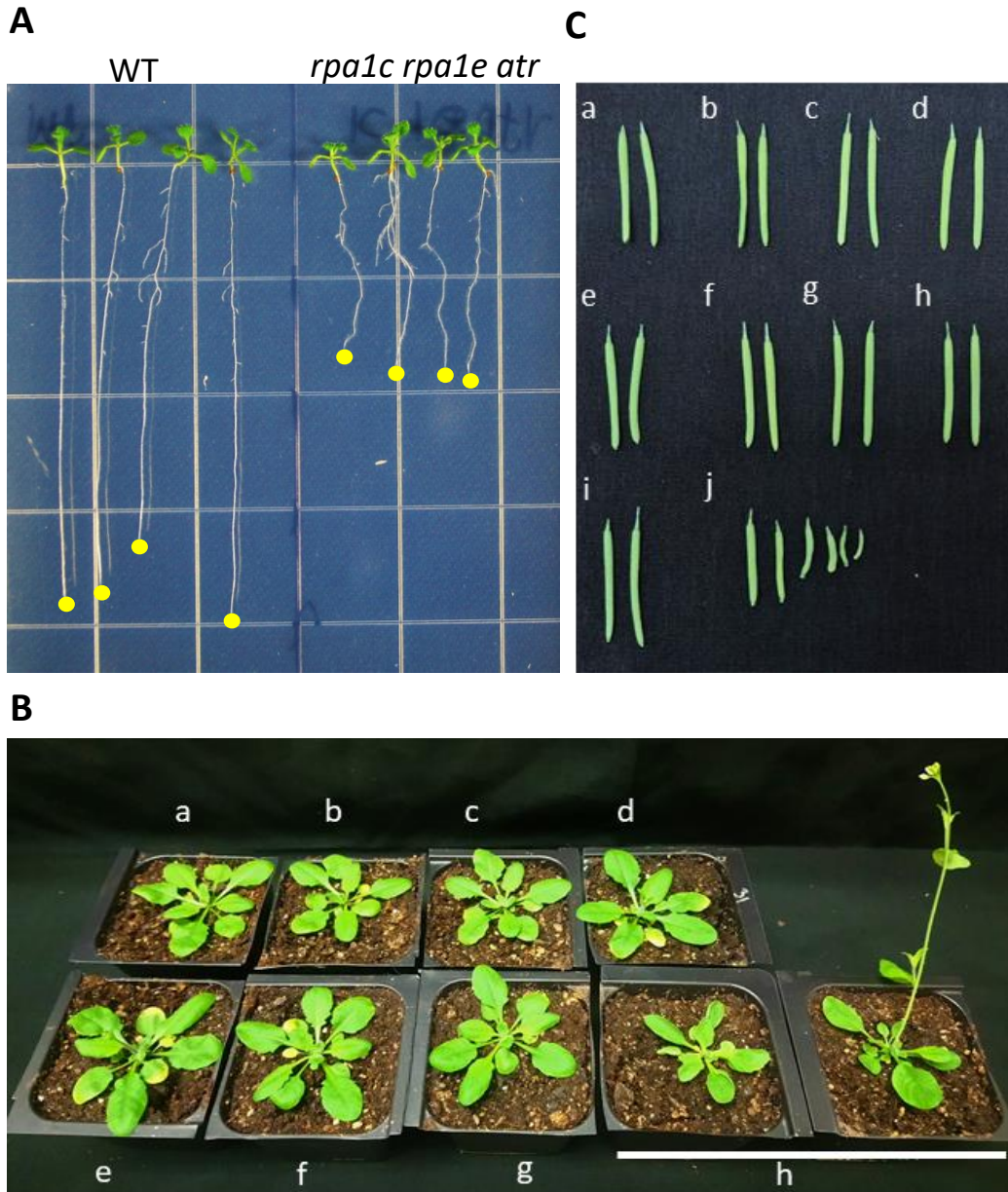
Supplementary Figure S5. AtTelo G4 structure. (A) FAM-At24-TAMRA displays G-quadruplex folding in sodium and potassium buffer. CD spectra at 4°C in NaCl (red), KCl (blue), and LiCl (green) at 3µM FAM-At24-TAMRA oligonucleotide strand concentration. (B) and (C) Thermal melting followed by FRET (excitation at 470 nm, emission at 520nm of FAM-At24-TAMRA oligonucleotide in NaCl (B) and KCl (C). Blue, red and green lines represent technical replicates. T_{1/2}: temperature of half-dissociation.



Supplementary Figure S6. RPA^{1B2A3B} binding on FAM-At24-TAMRA. FAM-At24-TAMRA (100nM) were incubated with different amounts of RPA1^{B2A3B} in the presence of 100 mM NaCl (Na⁺) or KCl (K⁺).



Supplementary Figure S7. ATR mutation partially rescues the short telomere phenotype in *rpa2a* mutant. Box plot (box = interquartile range, whiskers = range, X = mean, midline = median) indicates telomere length for WT and mutant lines from three independent biological replicates. Unpaired T-test was used to compare means. Asterisk denote statistically significant difference at $P \leq 0.05$.



Supplementary Figure S8. *ATR* mutation in *rpa1c rpa1e* backgrounds leads to defective growth and development. (A) 11-day-old seedlings showing a short root phenotype in *rpa1c rpa1e atr* triple mutants. Yellow dots indicate primary root tips. (B) Morphological phenotype of 30-day-old WT (a), *rpa1c* (b); *rpa1e* (c); *atr* (d); *rpa1c rpa1e* (e); *rpa1c atr* (f); *rpa1e atr* (g); and *rpa1c rpa1e atr* (h). The *rpa1c rpa1e atr* exhibits early flowering and curly and smaller rosette leaves phenotypes. All other mutants were similar to WT. (C) Siliques from 54-day-old plants. WT (a, e, i), *rpa1c* (b); *rpa1e* (c); *atr* (d); *rpa1c rpa1e* (f); *rpa1c atr* (g); *rpa1e atr* (h); *rpa1c rpa1e atr* (j). The short siliques in *rpa1c rpa1e atr* mutants reveal decreased fertility.